Induced Variations in Brassinosteroid Genes Define Barley Height and Sturdiness, and Expand the Green Revolution Genetic Toolkit[1][C][W][OPEN]

Christoph Dockter[2], Damian Gruszka[2], Ilka Braumann, Arnis Druka, Ilze Druka, Jerome Franckowiak, Simon P. Gough, Anna Janeczko, Marzena Kurowska, Joakim Lundqvist, Udda Lundqvist, Marek Marzec, Izabela Matyszczak, André H. Müller[3], Jana Oklestkova, Burkhard Schulz, Shakhira Zakhrabekova, and Mats Hansson[4]*

Carlsberg Laboratory, DK–1799 Copenhagen V, Denmark (C.D., I.B., S.P.G., J.L., I.M., A.H.M., S.Z., M.H.); Department of Genetics, Faculty of Biology and Environment Protection, University of Silesia, PL–40–032 Katowice, Poland (D.G., M.K., M.M.); James Hutton Institute, Invergowrie, Dundee DD2 5DA, United Kingdom (A.D., I.D.); Department of Agriculture, Fishery, and Forestry, Agri-Science Queensland, Hermitage Research Facility, Warwick, Queensland 4370, Australia (J.F.); Institute of Plant Physiology, Polish Academy of Sciences, 30–239 Krakow, Poland (A.J.); Nordic Genetic Resource Center, SE–230 53 Alnarp, Sweden (U.L.); Laboratory of Growth Regulators, Centre of the Region Haná for Biotechnological and Agricultural Research, Palacký University, and Institute of Experimental Botany, Academy of Sciences of the Czech Republic, CZ–783 71 Olomouc, Czech Republic (J.O.); and Department of Plant Science and Landscape Architecture, University of Maryland, College Park, Maryland 20742 (B.S.)

Reduced plant height and culm robustness are quantitative characteristics important for assuring cereal crop yield and quality under adverse weather conditions. A very limited number of short-culm mutant alleles were introduced into commercial crop cultivars during the Green Revolution. We identified phenotypic traits, including sturdy culm, specific for deficiencies in brassinosteroid biosynthesis and signaling in semidwarf mutants of barley (*Hordeum vulgare*). This set of characteristic traits was explored to perform a phenotypic screen of near-isogenic short-culm mutant lines from the *brachytic*, *breviaristatum*, *dense spike*, *erectoides*, *semibrachytic*, *semidwarf*, and *slender dwarf* mutant groups. In silico mapping of brassinosteroid-related genes in the barley genome in combination with sequencing of barley mutant lines assigned more than 20 historic mutants to three brassinosteroid-biosynthesis genes (*BRASSINOSTEROID-6-OXIDASE*, *CONSTITUTIVE PHOTOMORPHOGENIC DWARF*, and *DIMINUTO*) and one brassinosteroid-signaling gene (*BRASSINOSTEROID-INSENSITIVE1* [*HvBRI1*]). Analyses of F2 and M2 populations, allelic crosses, and modeling of nonsynonymous amino acid exchanges in protein crystal structures gave a further understanding of the control of barley plant architecture and sturdiness by brassinosteroid-related genes. Alternatives to the widely used but highly temperature-sensitive *uzu1.a* allele of *HvBRI1* represent potential genetic building blocks for breeding strategies with sturdy and climate-tolerant barley cultivars.

The introduction of dwarfing genes to increase culm sturdiness of cereal crops was crucial for the first Green Revolution (Hedden, 2003). The culms of tall cereal crops were not strong enough to support the heavy spikes of high-yielding cultivars, especially under high-nitrogen conditions. As a result, plants fell over, a process known as lodging. This caused losses in yield and grain-quality issues attributable to fungal infections, mycotoxin contamination, and preharvest germination (Rajkumara, 2008). Today, a second Green Revolution is on its way, to revolutionize the agricultural sector and to ensure food production for a growing world population. Concurrently, global climate change is expected to cause more frequent occurrences of extreme weather conditions, including thunderstorms with torrential rain and strong winds, thus promoting cereal culm breakage (Porter and Semenov, 2005; National Climate Assessment Development Advisory Committee, 2013). Accordingly, plant architectures that resist lodging remain a major crop-improvement goal and identification of genes that regulate culm length is required to enhance the genetic toolbox in order to facilitate efficient marker-assisted breeding. The mutations and the corresponding genes

that enabled the Green Revolution in wheat (*Triticum aestivum*) and rice (*Oryza sativa*) have been identified (Hedden, 2003). They all relate to gibberellin metabolism and signal transduction. It is now known that other plant hormones such as brassinosteroids are also involved in the regulation of plant height. Knowledge of the molecular mechanisms underlying the effects of the two hormones on cell elongation and division has mainly come from studies in Arabidopsis (*Arabidopsis thaliana*; Bai et al., 2012). Mutant-based breeding strategies to fine-tune brassinosteroid metabolism and signaling pathways could improve lodging behavior in modern crops (Vriet et al., 2012) such as barley (*Hordeum vulgare*), which is the fourth most abundant cereal in both area and tonnage harvested (http://faostat.fao.org).

A short-culm phenotype in crops is often accompanied by other phenotypic changes. Depending on the penetrance of such pleiotropic characters, but also the parental background and different scientific traditions and expertise, short-culmed barley mutants were historically divided into groups, such as *brachytic* (*brh*), *breviaristatum* (*ari*), *dense spike* (*dsp*), *erectoides* (*ert*), *semibrachytic* (*uzu*), *semidwarf* (*sdw*), or *slender dwarf* (*sld*; Franckowiak and Lundqvist, 2012). Subsequent mutant characterization was limited to intragroup screens and very few allelism tests between mutants from different groups have been reported (Franckowiak and Lundqvist, 2012). Although the total number of short-culm barley mutants exceeds 500 (Franckowiak and Lundqvist, 2012), very few have been characterized at the DNA level (Helliwell et al., 2001; Jia et al., 2009; Chandler and Harding, 2013; Houston et al., 2013). One of the first identified haplotypes was uzu barley (Chono et al., 2003). The *Uzu1* gene encodes the brassinosteroid hormone receptor and is orthologous to the *BRASSINOSTEROID-INSENSITIVE1* (*BRI1*) gene of Arabidopsis, a crucial promoter of plant growth (Li and Chory, 1997). The *uzu1.a* allele has been used in East Asia for over a century and is presently distributed in winter barley cultivars in Japan, the Korean peninsula, and China (Saisho et al., 2004). Its agronomic importance comes from the short and sturdy culm that provides lodging resistance, and an upright plant architecture that tolerates dense planting.

Today, more than 50 different brassinosteroids have been identified (Bajguz and Tretyn, 2003). Most are intermediates of the complex biosynthetic pathway (Shimada et al., 2001). Approximately nine genes code for the enzymes that participate in the biosynthetic pathway from episterol to brassinolide (Supplemental Fig. S1). Brassinosteroid deficiency is caused by downregulation of these genes, but it can also be associated with brassinosteroid signaling. The first protein in the signaling network is the brassinosteroid receptor encoded by *BRI1* (Li and Chory, 1997; Kim and Wang, 2010). In this work, we show how to visually identify brassinosteroid-mutant barley plants and we describe more than 20 relevant mutations in four genes of the brassinosteroid biosynthesis and signaling pathways that can be used in marker-assisted breeding strategies.

RESULTS

Phenotypic Identification of Brassinosteroid Mutants in Barley

A large number of *brh*, *ari*, *dsp*, *ert*, *uzu*, *sdw*, and *sld* short-culm mutants have been induced in various barley cultivars, and many mutants within each group were found to be allelic (Franckowiak and Lundqvist, 2012). We hypothesized that mutants from different groups might be allelic too; however, because of their different genetic backgrounds, direct comparison of their mutant phenotypes was impossible. Representative lines from these groups, along with many other mutants, were recently crossed into the genetic background of barley 'Bowman' and genotyped with up to 3,000 markers (Druka et al., 2011). By growing such near-isogenic lines in parallel in the same environment, we were able to perform a comprehensive comparison of their mutant phenotypes independently of their original genetic background or preconceptions derived from previous historic classification (Fig. 1).

The brassinosteroid receptor, encoded by *Uzu1* (*HvBRI1*), is known to regulate plant height in barley (Chono et al., 2003). We used BW885, the near-isogenic line carrying the *uzu1.a* allele (Druka et al., 2011), as an ideotype for a barley brassinosteroid mutant. When grown at low temperatures, the *uzu1.a* mutant is a semidwarf with 80% of wild-type culm length (Fig. 2). The elongation of upper-stem internodes is particularly reduced while the stem diameter remains unaltered. The overall plant architecture is more erect, with acute leaf-blade angles. Short-awned spikes are compact with dense basal spikelets, and frequently with opposite spikelets in the tip caused by irregular elongation of rachis internodes. Leaf margins and auricles of *uzu1.a* have a slightly undulating appearance, similar to the wavy leaf phenotype found in maize (*Zea mays*) *Wavy auricle in blade1* mutants (Hay and Hake, 2004). The same phenotypic detail, but to a more extreme extent, was found in cv Bowman wild-type plants treated with propiconazole (Fig. 2), a potent inhibitor of brassinosteroid biosynthesis (Hartwig et al., 2012). In anatomical and microscopic analyses, we found other phenotypic details (Supplemental Fig. S2).

We used the unique combination of visible brassinosteroid-mutant characters once they were established to perform a phenotypic screen of 160 cv Bowman near-isogenic lines with reduced culm length. Sixteen lines fulfilled the brassinosteroid phenotype criteria. These mutants were found in the *brh*, *uzu*, *ari*, and *ert* groups (Fig. 3). We also tested the response of dark-grown seedling leaves to exogenously applied brassinolide (Honda et al., 2003), in order to differentiate potential brassinosteroid-signaling mutants from those with impaired brassinosteroid biosynthesis. In this so-called leaf-unrolling test, the mutants were grown in darkness for 6 d at 26°C and tightly rolled leaf segments were immersed in water or in a solution containing the most active brassinosteroid, brassinolide, for 72 h. Mutants *ari.256*, *ert-ii.79*, and *uzu1.a* showed greatly reduced

Figure 1. Main barley complementation groups in the cv Bowman near-isogenic line collection, which contain mutants with a short-culm phenotype. Gross morphology of representatives of the barley mutant groups *brh, ari, dsp, ert, uzu, sdw,* and *sld* compared with cv Bowman. Scale bar = 10 cm. [See online article for color version of this figure.]

Bowman   *brh18.ac*   *ari-c.2*   *dsp10.ba*   *ert-zd.159*   *uzu1.a*   *sdw.at*   *sld2.b*
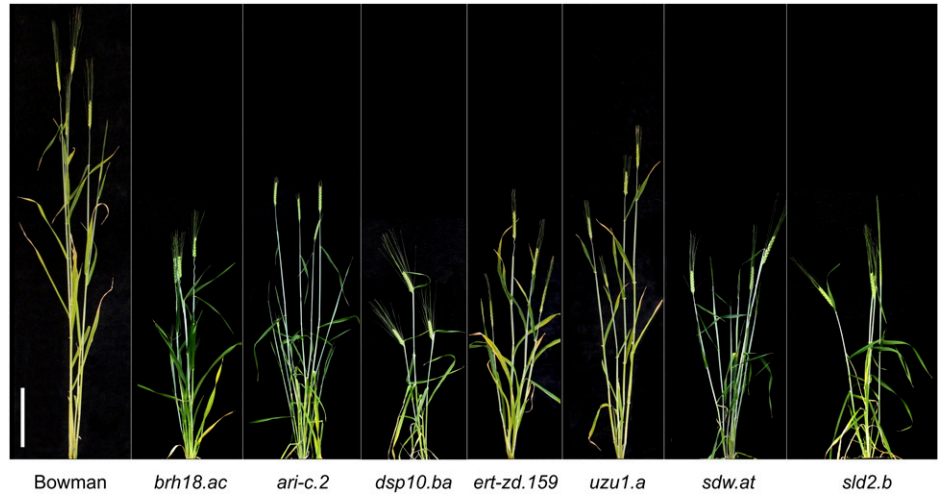
leaf-unrolling response to brassinolide (Fig. 3D), suggesting defective brassinosteroid signaling. In rice, a leaf lamina inclination assay has been successfully used to identify brassinosteroid signaling mutants (Fujioka et al., 1998; Hong et al., 2003). We adopted this method to barley. Addition of brassinolide to the tip of barley seedlings resulted in an increased angle between the first leaf blade and culm in wild-type plants and those mutants that responded to exogenously applied brassinolide. Mutants insensitive in the leaf-unrolling assay also missed increased leaf inclination, an indication for a defect in brassinosteroid signaling (Supplemental Fig. S3).

In order to test the robustness of the brassinosteroid-deficient characters for direct phenotypic screening, we studied 950 M2 plants of a chemically mutagenized doubled-haploid population of the barley line H930-36. Of 16 candidate plants with short-culm phenotypes, one showed the specific brassinosteroid-deficient characters. In the leaf-unrolling test, the mutant leaf segments showed reduced response to added brassinolide (Fig. 4, A–F). Thus, the mutant was grouped with *ari.256, ert-ii.79,* and *uzu1.a,* and selected for further analysis of the brassinosteroid-signaling gene, *HvBRI1*.

Connecting Brassinosteroid Biosynthesis Genes with Barley Mutant Loci

A rich variety of brassinosteroids are intermediates of the complex biosynthetic pathway (Supplemental Fig. S1). After initial steps, the pathway branches into an early or late C-6 oxidation route. Several enzymes have broad substrate specificity. Therefore, they catalyze multiple steps of the pathway. The final product is brassinolide, which is generated by conversion from castasterone. The oxidase catalyzing the final step has not been found in cereal grasses, like barley. In these plants, castasterone was suggested to be the bioactive end product of the brassinosteroid biosynthetic pathway (Kim et al., 2008). We identified nine genes encoding enzymes of the pathway in the barley genome by homology searches between deduced polypeptide sequences of barley and Arabidopsis (Supplemental Fig. S4). These were mapped on the barley genome in silico using the barley genome zipper (Mayer et al., 2011) and the barley physical map (The International Barley Genome Sequencing Consortium, 2012). The genomic locations were then compared with the mutant

Figure 2. The brassinosteroid phenotype of the cv Bowman near-isogenic line BW885 (*uzu1.a*) compared with wild-type cv Bowman (Bow). A, Gross morphology and overall plant architecture. B and C, Awns and spikes are short with reduced rachis-internode length at the base and tip. D and E, Leaves are erect with undulating leaf margins. The latter phenotype was also found in wild-type cv Bowman grown in the presence of the brassinosteroid-biosynthetic inhibitor propiconazole (PCZ). Scale bars = 10 cm. [See online article for color version of this figure.]
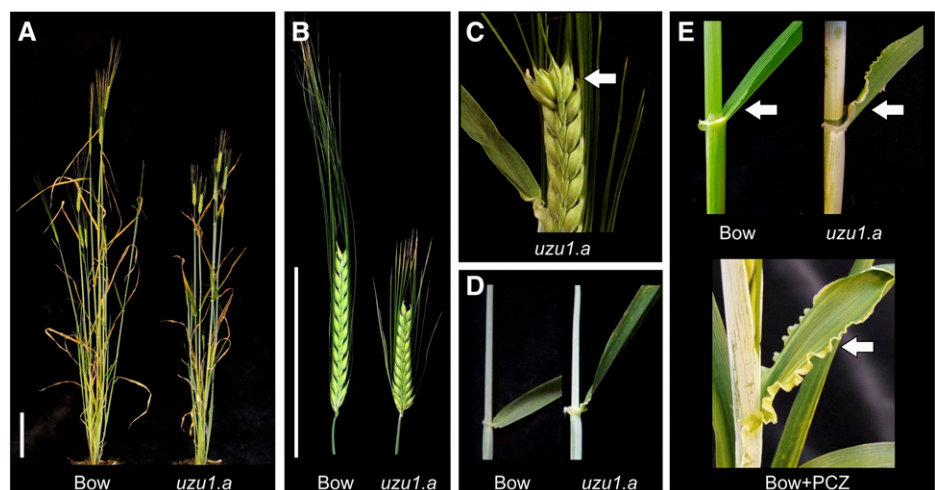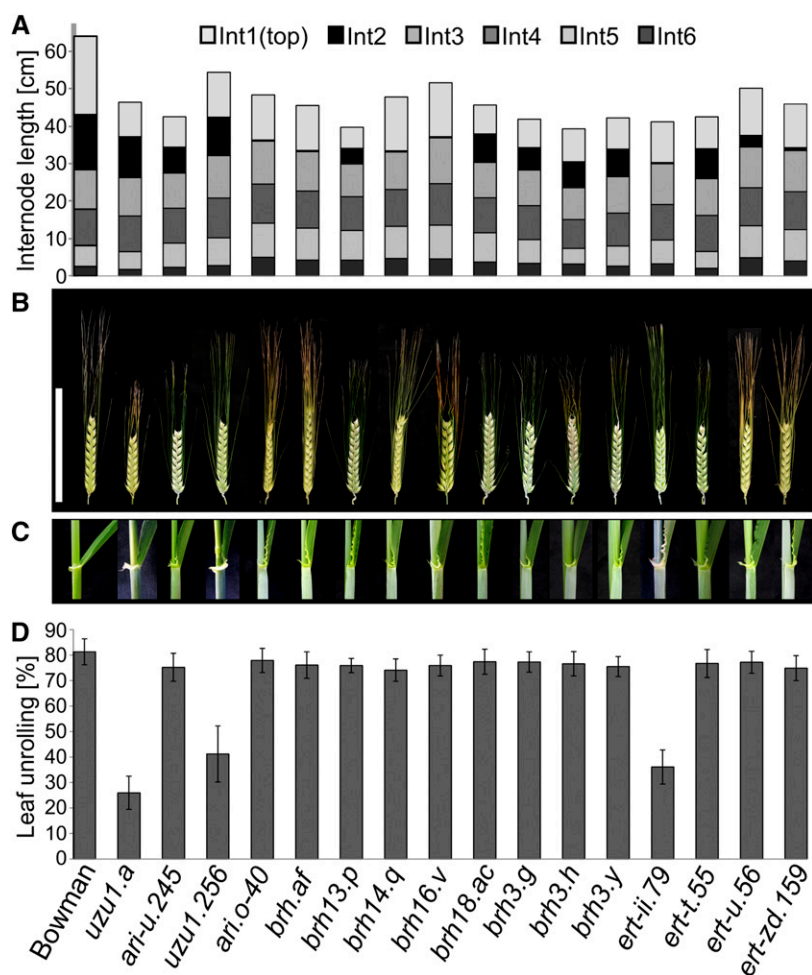
Figure 3. Phenotypic details of mutants in the collection of cv Bowman near-isogenic lines with an *uzu1.a*-like plant architecture. A, Reduced culm length due to short upper internodes. B, Irregular rachis-internode length and short awns. C, Acute leaf angles and undulating leaf margins. D, Insensitivity to exogenously applied brassinolide (*uzu1.a*, *uzu1.256*, and *ert-ii.79*) in a leaf-unrolling bioassay is indicative of defects in brassinosteroid signaling. Mutant *uzu1.256* was renamed from its previous name *ari.256*. Scale bar = 10 cm. [See online article for color version of this figure.]

donor introgressions of the selected near-isogenic lines, which suggest that the mutants are alleles of three biosynthetic genes, (*BRASSINOSTEROID-6-OXIDASE* [*HvBRD*], *CONSTITUTIVE PHOTOMORPHOGENIC DWARF* [*HvCPD*], and *DIMINUTO* [*HvDIM*]), or of the brassinosteroid receptor gene *HvBRI1* (Fig. 5). This was tested by sequencing of the genes from available near-isogenic lines and historic barley mutants, and by performing allelic crosses.

Genetic Characterization of *HvBRD* Mutants

HvBRD, encoding a brassinosteroid-6-oxidase, is located in the telomeric region of the short arm of barley chromosome 2H (Fig. 5; Supplemental Fig. S5A). The location of *HvBRD* is within the mutant donor introgressions of the near-isogenic lines *ari-u.245*, *brh3.g*, *brh3.h*, *brh3.y*, and *ert-t.55*. In the barley genome zipper, the common genetic donor interval of those lines contained 21 gene models but did not include the *HvBRD* ortholog of *Brachypodium distachyon*, rice, and sorghum (*Sorghum bicolor*). In EnsemblPlant (http://plants.ensembl.org), the same interval contained 68 gene models including *HvBRD*. Sequencing of *HvBRD* identified nonsense

mutations in *ari-u.245* (T1676A, Leu-257 replaced by stop), *brh3.g*, and *brh3.h* (G2723A, Trp-444 replaced by stop), and a point mutation in *brh3.y* (G2183A) causing a Gly-353 to Asp modification in the dioxygen-binding site of *HvBRD* (Fig. 6; Supplemental Fig. S5B; Supplemental Data Set S1). Allelism between available *brh3* and *ert-t* loci was recently proven (Dahleen et al., 2005; Franckowiak and Lundqvist, 2012). In this study, we additionally verified the allelic nature of *ari-u.245* to the *brh3* and *ert-t* groups by a cross between *ari-u.245* and *brh3.y*. The F1 progeny, heterozygous for the parental mutations in *HvBRD*, clearly resembled the brassinosteroid-deficient phenotype (Fig. 7A). We also identified mutations in *brh3.i* and *ert-t.437*, which have been reported as allelic mutants (Dahleen et al., 2005) but are not represented in the collection of near-isogenic lines. The nonsense mutation in *brh3.i* was identical to *brh3.g* and *brh3.h*, and the point mutation in *ert-t.437* was identical to *brh3.y*. Other genetic differences in *HvBRD* clearly indicate an independent history of *ert-t.437* and *brh3.y* (Supplemental Data Set S1). No mutation within the coding region of *HvBRD* could be found in BW324 (*ert-t.55*) or the original *ert-t.55* mutant, even though the mutant was reported allelic to *brh3* mutants (Dahleen et al., 2005) and to *ert-t.437* (Franckowiak and Lundqvist,
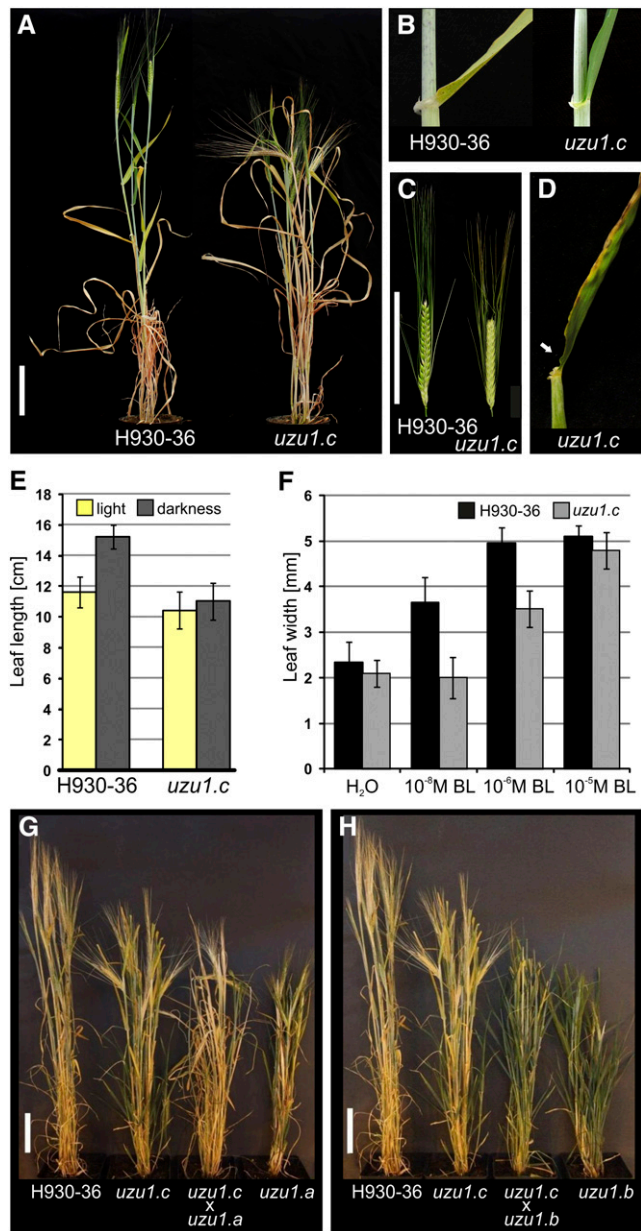
Figure 4. Phenotypic characterization of the *HvBRI1* allele *uzu1.c* compared with the double-haploid line H930-36. A, Gross morphology and overall plant architecture with reduced culm length. B, Acute leaf angles. C, Awns and spikes are short with reduced rachis-internode length. D, Undulated leaf margins. E, Reduced leaf elongation under dark growing conditions. F, Reduced sensitivity to exogenously applied brassinolide (BL) in a leaf-unrolling bioassay. G and H, Gross morphology of *HvBRI1* alleles *uzu1.a, uzu1.b, uzu1.c,* and their respective F1 progeny of allelism crosses. Scale bars = 10 cm. [See online article for color version of this figure.]

2012). We therefore suggest that the *ert-t.55* mutation is located outside the sequenced region of *HvBRD*, possibly in a regulatory element, or that the mutation has caused a rearrangement in the telomeric region of chromosome 2H, not detectable in our experimental setup. Mutant *ert-t.55* was induced by x-ray treatment (Supplemental Data Set

S1). BW093, the presumed near-isogenic line of *brh3.i*, neither had an introgression on chromosome 2H (Druka et al., 2011) nor harbored the *brh3.i* haplotype although it showed a short-culm phenotype (Supplemental Data Set S1). In contrast with the original line *brh3.i*, BW093 was also missing the combination of brassinosteroid-mutant characters, indicating a diverse ancestry of the genotypes. The connection between mutations in *HvBRD* and the brassinosteroid-deficient phenotype, was further strengthened by an exact cosegregation of the phenotype with the *brh3.g* allele in an F2-mapping population. That is, 103 plants genotyped as homozygous *brh3.g* mutants all had a short awn length (range, 4.5–8.1 cm; average ± SD, 6.8 ± 0.81 cm) in contrast with the long awn lengths of 190 heterozygous mutants (10.5–14.6 cm; 12.6 ± 0.84 cm) and 90 wild-type plants (11.4–15.0 cm; 12.8 ± 0.90 cm).

Genetic Characterization of *HvCPD* Mutants

HvCPD, encoding the barley C-23α-hydroxylase cytochrome P450 90A1 (CYP90A1), could not be localized on the physical map of the barley genome. Instead, the synteny to *B. distachyon*, rice, and sorghum genomes (Mayer et al., 2011) was used to identify likely markers for *HvCPD*. Among mutants with a brassinosteroid-deficient phenotype, only *brh13.p* has an introgression region (Druka et al., 2011) colocalizing with the suggested position of *HvCPD* at 44.24 centimorgans (cM) on chromosome 5H (Fig. 5; Supplemental Fig. S6A). However, the introgression region of *brh13.p* is large and supposed to contain 1,380 gene models according to the barley genome zipper (Mayer et al., 2011) and 808 gene models according to EnsemblPlant (http://plants.ensembl.org) but only one brassinosteroid-biosynthesis gene, *HvCPD*. The near-isogenic line of *brh18.ac* was not included in the marker analysis by Druka et al. (2011), but *brh18.ac* has previously been linked to *brh13.p* via the Simple Sequence Repeat markers Bmag0387 and *HvLEU* (Dahleen et al., 2005). The latter is anchored approximately 6 cM from *HvCPD*. We performed a cross between mutant lines *brh13.p* and *brh18.ac*. The F1 progeny, heterozygous for the parental mutations in *HvCPD*, clearly displayed a brassinosteroid-mutant phenotype, verifying that *brh13.p* and *brh18.ac* are allelic (Fig. 7B). Sequencing of *HvCPD* showed *brh13.p* and *brh18.ac* to carry point mutations (C2562T and C2807T, respectively) causing substitutions of highly conserved amino acid residues (Pro-445 to Leu in *brh13.p* and Pro-479 to Ser in in *brh18.ac*). Pro-445 and Pro-479 are located within and close to the highly conserved heme binding site, respectively, in the C-terminal part of *HvCPD* (Fig. 6; Supplemental Fig. S6B; Supplemental Data Set S1). It was noted that 11 additional near-isogenic lines with a short-culm phenotype, but without other distinct brassinosteroid-mutant characters, have overlapping introgression regions with *HvCPD* (Supplemental Data Set S1). Sequencing of *HvCPD* from these 11 lines revealed no mutations, which suggests that they are not deficient in *HvCPD*.
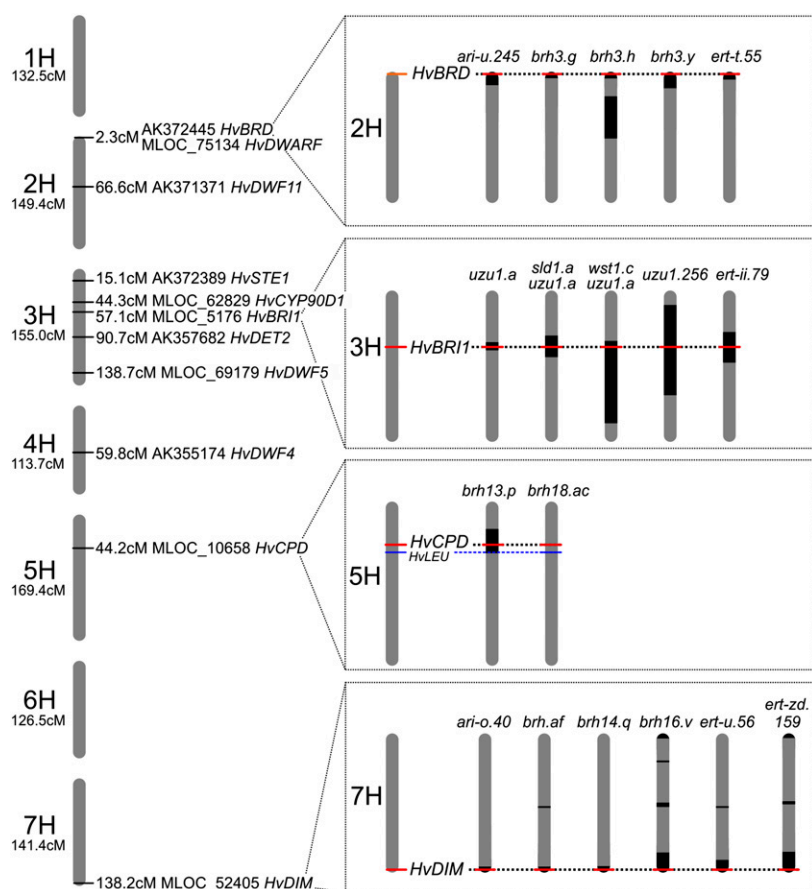
Figure 5. In silico mapping of brassinosteroid biosynthesis genes and receptor gene *HvBRI1* revealed mutant candidates in the collection of cv Bowman near-isogenic lines. MLOC-gene positions on barley chromosomes (gray) according to the barley genome map (The International Barley Genome Sequencing Consortium, 2012); mutant donor introgressions (black) according to Druka et al. (2011). Loci *HvDET2* and *HvCPD* are not anchored in the barley genome map, but were localized in the barley genome zipper (Mayer et al., 2011). [See online article for color version of this figure.]

Genetic Characterization of *HvDIM* Mutants

The sequence of *HvDIM*, encoding the barley Δ^5-sterol-Δ^{24}-reductase DIMINUTO, corresponds directly to single-nucleotide polymorphism (SNP) marker 1_0547 in the telomere on the long arm of chromosome 7H. The six near-isogenic lines of *ari-o.40*, *brh.af*, *brh14.q*, *brh16.v*, *ert-u.56*, and *ert-zd.159* have a small, common genetic donor interval containing the *HvDIM* locus (Fig. 5; Supplemental Fig. S7A). In addition, the six mutants show a brassinosteroid-deficient phenotype including a short culm mainly caused by a specific and extreme shortening of the second culm internode (Fig. 3A). In the barley genome zipper (Mayer et al., 2011), the interval contained three gene models including the *HvDIM* ortholog of *B. distachyon*, rice, and sorghum. In EnsemblPlant (http://plants.ensembl.org), the same interval contained 27 gene models. Severe DNA changes were identified in the six mutants (Supplemental Data Set S1). In *brh14.q*, induced by ethyl methanesulfonate treatment, a C628T substitution was detected resulting in the exchange of Leu-210 to Phe in the highly conserved FAD-binding site. Mutation *ert-zd.159* was found in the same domain (A530T, Glu-177 to Val), whereas the mutant *ari-o.40* had a T1171A substitution resulting in a Trp-391 to Arg exchange. Although Trp-391 is located in a domain of unknown function, Trp-391 is highly conserved among plant DIM polypeptides and

also in comparison to the human ortholog of DIM, SELADIN-1 (Supplemental Fig. S7B; Greeve et al., 2000). The deletions found in *brh16.v* (C3937 deleted, causing a frame shift followed by a premature stop codon), *ert-u.56* (exon 1 deleted, induced by x-rays), and *brh.af* (deletion of >12 kb, induced by neutrons) further verified *HvDIM* as the candidate gene. Crosses generated F1 progenies with identical phenotypes to their parental lines, verifying the allelic character of the gene loci (Fig. 7C). In addition to *ari-o.40*, six other alleles of *ari-o* are available. *HvDIM* mutations in *ari-o.43* and *ari-o.143* were identical to *ari-o.40*, whereas no mutations in *HvDIM* were found in *ari-o.297*, *ari-o.301*, *ari-o.304*, and *ari-o.306* even though they showed a brassinosteroid-deficient phenotype. Crosses of *ari-o.297*, *ari-o.301*, *ari-o.304*, and *ari-o.306* to *ari-o.40* resulted in F1 progenies with a tall wild-type phenotype without brassinosteroid-mutant characters (Fig. 7D). This confirmed that *ari-o.297*, *ari-o.301*, *ari-o.304*, and *ari-o.306* are wrongly annotated alleles of *HvDIM*. Sequencing the latter four lines for *HvCPD*, *HvBRD*, and *HvBRI1* identified three mutants: nonsynonymous point mutations in *HvBRI1* in *ari-o.297* (T158C, Phe-53 to Ser; renamed *uzu1.297*) and *ari-o.301* (T845A, Val-282 to Asp; renamed *uzu1.301*), and a nonsense mutation in *HvBRD* in *ari-o.304* (A2736T; Lys-449 replaced by stop; renamed *ari-u.304*; Fig. 6). No mutation was found in *ari-o.306* (renamed *ari.306*).

Figure 6. Structures of analyzed brassinosteroid genes. A, HvBRD. B, HvCPD. C, HvDIM. D, HvBRI1. The location and number of exons (E) and the identity of mutations at the gene and peptide levels (three letter code, italic) are indicated. Dotted lines in C represent deleted gene fragments in the respective mutant accessions. Asterisks indicate nonsense mutations where amino-acid residues have been exchanged by stop.
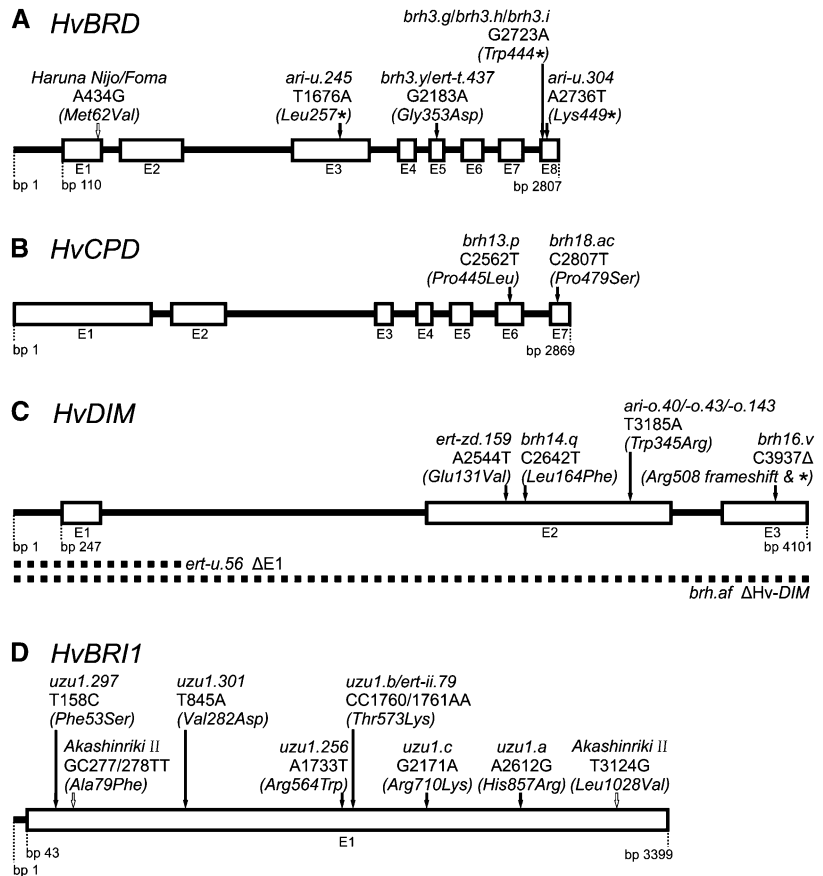
Genetic Characterization and Novel Alleles of HvBRI1

In addition to the uzu1 standard line BW885, the reported uzu1.a mutation (Chono et al., 2003) is also present in BW860 (sld1.a + uzu1.a) and BW912 (wst1.c + uzu1.a). These three near-isogenic lines delimit the HvBRI1 position to a shared interval covered by nine SNPs on chromosome 3H (Fig. 5; Supplemental Fig. S8A). This interval contained 150 gene models according to EnsemblPlant (http://plants.ensembl.org) and 217 gene models according to the barley genome zipper, including the BRI1 ortholog of B. distachyon, rice, and sorghum. Sequencing of HvBRI1 from those lines revealed the expected single substitution A2612G (His-857 to Arg), known as allele uzu1.a, which is found in Northeast Asian short-culm cultivars and landraces such as 'Akashinriki' (Chono et al., 2003; Supplemental Data Set S1).

HvBRI1 is also located within the introgression regions of near-isogenic lines ari.256 and ert-ii.79 (Supplemental Fig. S8A), which, like BW885 (uzu1.a), showed a brassinosteroid signaling-deficient phenotype in a leaf-unrolling test (Fig. 3D). Sequencing of HvBRI1 revealed mutations in both ari.256 (A1733T; renamed uzu1.256) and ert-ii.79 (C1760A and C1761A; Fig. 6; Supplemental Fig. S8B; Supplemental Data Set S1). The amino acid residues affected by the mutations in uzu1.256 (Arg-564 to Trp) and ert-ii.79 (Thr-573 to

Lys) are located in the region encoding the steroid-binding island domain (Fig. 8, A and B). The introduction of the charged Lys-573 to the hydrophobic active site surrounding residues, destroying charge neutrality, is expected to prevent brassinosteroid binding. In both cases, steric clashes with neighboring residues are likely to occur (Fig. 8B, inserts); as a consequence, the steroid binding and the general positioning of the brassinosteroid-binding site may be affected. Alternatively, the change in the surface polarity (Fig. 8, C and D) in the putative docking site of BRASSINOSTEROID INSENSITIVE1-ASSOCIATED RECEPTOR KINASE1 (BAK1) and other SOMATIC EMBRYOGENESIS RECEPTOR KINASE (SERK)-like coreceptors (Fig. 8C, yellow circle) may simply hinder the BRI1-SERK interaction, although less severe than in Arabidopsis bri1-102 (AtThr750 to Ile), which is a strong dwarf mutant (Supplemental Fig. S8B; Hothorn et al., 2011; She et al., 2011; Sun et al., 2013). By using the Arabidopsis BAK1/SERK3 (AT4G33430) sequence as probe, we identified at least five SERK-like barley genes (MLOC_19580, AK252995 [identical to MLOC_80630 and MLOC_59982], MLOC_8229, MLOC_6922, and MLOC_79186) in available barley sequence databases (IPK Barley BLAST Server, http://webblast.ipk-gatersleben.de/). Their specific functions in barley are not yet known, but they are likely to form a BRI1/
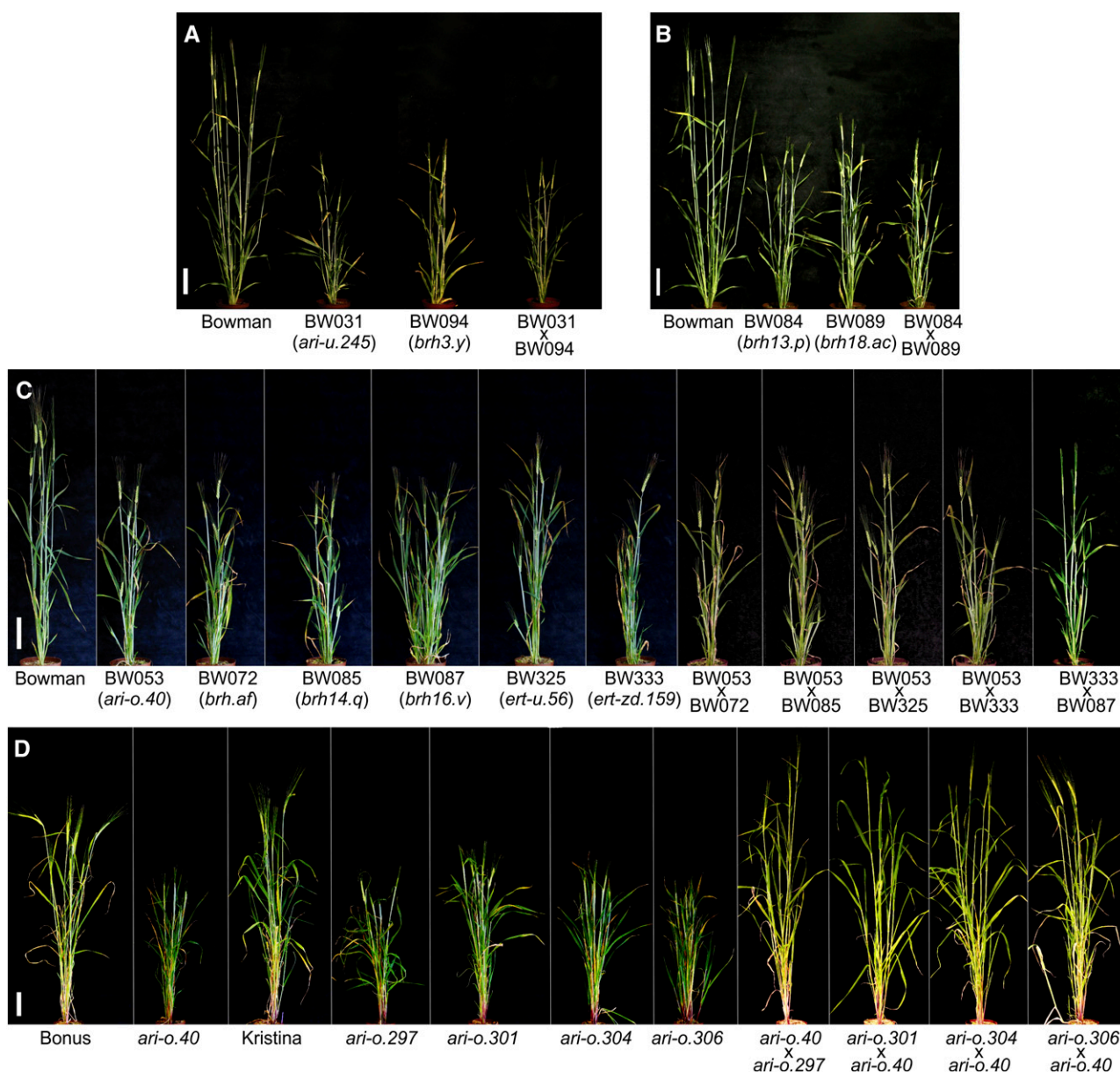
Figure 7. Allelism crosses. A, Gross morphology of putative *HvBRD* mutants BW031 (*ari-u.245*), BW094 (*brh3.y*), and the F1 progeny of a cross BW031 × BW094. B, Gross morphology of putative *HvCPD* mutants BW084 (*brh13.p*), BW089 (*brh18.ac*), and the F1 progeny of a cross BW084 × BW089. C, Gross morphology of putative *HvDIM* mutants BW053 (*ari-o.40*), BW072 (*brh.af*), BW085 (*brh14.q*), BW087 (*brh16.v*), BW325 (*ert-u.56*), and BW333 (*ert-zd.159*) and their respective F1 progeny of allelism crosses. D, Gross morphology of wild-type cv Bonus and cv Kristina, original *ari-o* alleles and their respective F1 progeny of allelism crosses. Scale bars = 10 cm. [See online article for color version of this figure.]

SERK heterodimer by docking to the brassinosteroid binding island domain in the BRI1 ectodomain (Fig. 8C, marked area; Sun et al., 2013).

More than 30 additional near-isogenic lines with a short-culm or spike morphology phenotype, but without the unique combination of brassinosteroid-mutant characters, have overlapping introgression regions with *HvBRI1*. Five of eight mutants induced in 'Steptoe' carried a 4-bp and a 1-bp deletion in the 3′ untranslated region and two of four mutants induced

in 'Akashinriki'-derived lines carried the same deletions plus three nucleotide substitutions that caused two nonsynonymous changes of amino acid residues (Ala-79 to Phe and Leu-1028 to Val) in the BRI1 N- and C-terminal domains, respectively (*AkashinrikiII*-allele; Chono et al., 2003). None of those haplotypes displayed an obvious brassinosteroid phenotype (Supplemental Data Set S1), which suggests that they are not deficient in *HvBRI1*. Haplotypes 6 and 7 were found in the wrongly annotated *ari-o* alleles *uzu1.297* and *uzu1.301*

Figure 8. Structural basis of brassinosteroid perception and signaling in barley *HvBRI1* mutants. A to D, X-ray structure of the Arabidopsis BRI1 brassinosteroid-binding domain (Protein Data Bank accession no. 3RGZ; Hothorn et al., 2011; She et al., 2011) displayed as ribbon (A and B) and hydrophobicity (C and D) models, respectively. LRRs missing in monocots are shown in white, the brassinosteroid-binding site (island domain) in yellow, and the bound steroid hormone brassinolide in red. E and F, X-ray structure of the Arabidopsis BRI1 kinase domain (Protein Data Bank accession no. 4OAB). The two views are rotated 90° relative to each other. BRI1 in complex with ATP (red), the BRI1 activation loop with phosphorylation sites (in yellow), and the proposed protein-docking platform for the BRI1 inhibitor BKI or the SERK coreceptors (circled) are highlighted (Bojar et al., 2014). The numbering of amino acid residues refers to the barley peptide sequence shown in Supplemental Figure S8B online in which corresponding residue positions in Arabidopsis AtBRI1 or rice OSBRI1 are indicated. Protein structures were visualized using Chimera software (Pettersen et al., 2004).
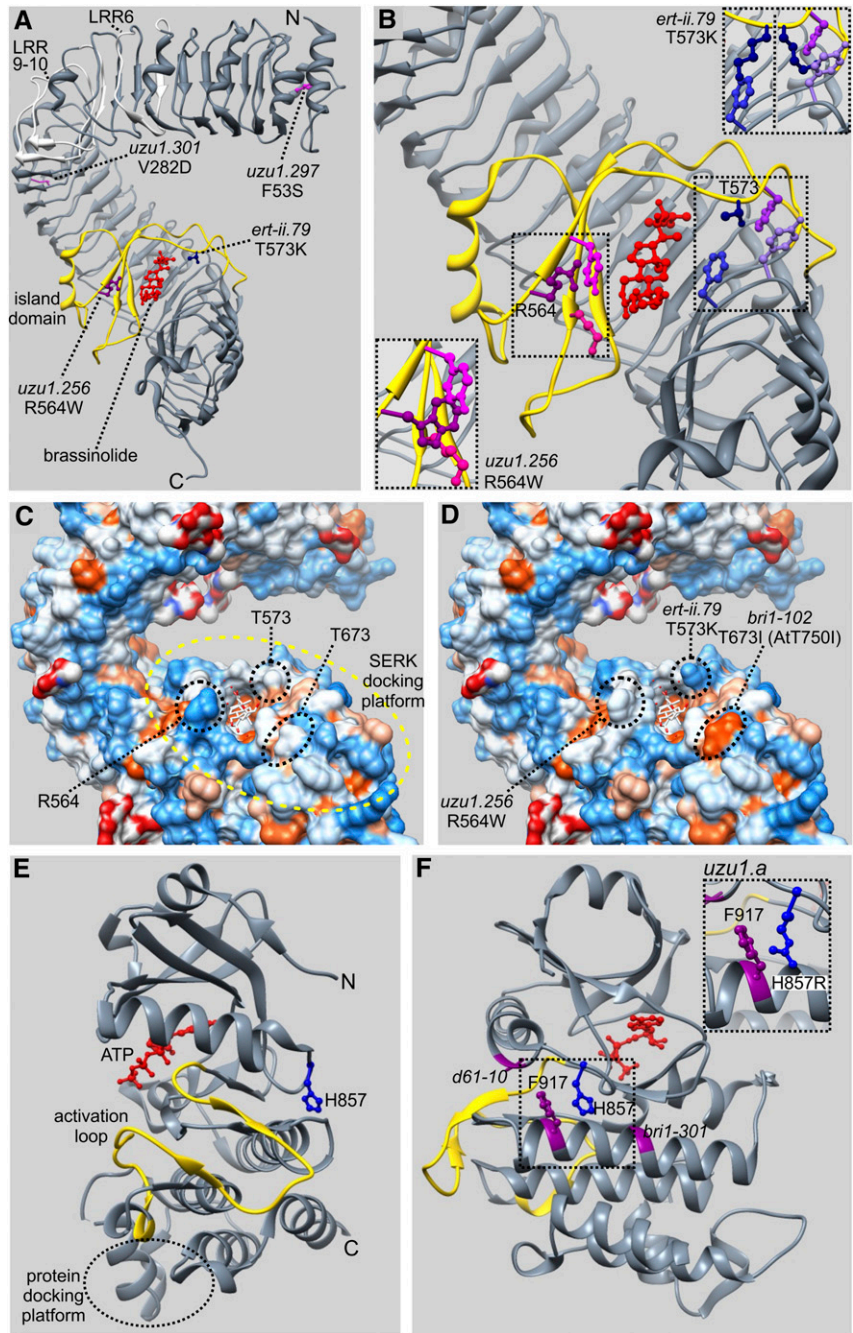
(Fig. 7D). The amino acid exchange found in *uzu1.297* (Phe-53 to Ser; Fig. 8A) is located within the C lobe of the N-terminal cap (Hothorn et al., 2011). The exchange to Ser-53 may destabilize the structure of this domain causing endoplasmic reticulum retention of BRI1 (Hong et al., 2008). The exchange of the nonpolar Val-282 residue to the negatively charged Asp in *uzu1.301* will result in the formation of a salt bridge between Asp-282 and Lys-302 (α-C distance 4.46Å), which may destabilize the structure of the folded protein due to a loss of solvation energy of Lys-302, which is solvent exposed (Bosshard et al., 2004). Alternatively, the exchange of the nonpolar

Val-282 to the negatively charged Asp may inhibit the superhelical arrangement (Ile-Pro spine) in leucine-rich repeat (LRR)-12 and thus cause a repositioning of the upstream LRRs and the N-terminal cap (Hothorn et al., 2011; Santiago et al., 2013).

Interestingly, the *ert-ii.79* mutation was identified earlier in the *uzu1* mutant *093AR* (*uzu1.b*; Gruszka et al., 2011b). To exclude a common ancestry between *093AR* and *ert-ii.79*, we genotyped the original accessions using 383 Amplified Fragment Length Polymorphism (AFLP) markers. We found a high level of polymorphism (7.6%) throughout the genomes,

indicating independent mutagenic events. The phenotypic characteristics of *uzu1.b* could be seen in all three genetic backgrounds (Fig. 9), supporting the robustness of the brassinosteroid-deficient characters for direct phenotypic screening of barley mutant collections.

Sequencing of *HvBRI1* from the brassinosteroid-insensitive mutant isolated among the 950 M2 plants of a chemically mutagenized population derived from the doubled-haploid line H930-36, revealed a novel *HvBRI1* allele (a single-nucleotide G2171A substitution), which we named *uzu1.c* (Fig. 6; Supplemental Fig. S8B; Supplemental Data Set S1). Cosegregation of genotype and phenotype in M3 plants and allelism tests with both *uzu1.a* and *uzu1.b* verified the new *uzu1* haplotype (Fig. 4, G and H). Substitution of the semiconserved Arg-710

to Lys in close proximity to the BRI1 transmembrane-binding domain causes a mild brassinosteroid phenotype. No other mutations were found in *HvBRI1* among the remaining 949 M2 plants. The successful identification of the *HvBRI1* mutant in a chemically induced mutant population and the clear brassinosteroid phenotypes seen in crosses and in different genetic backgrounds (Figs. 4, 7, and 9) strongly suggest that brassinosteroid phenotypes are identifiable in mutant populations of most barley cultivars.

Temperature Sensitivity of *uzu1.a*

The *uzu1.a* allele, widely distributed in Northeast Asian winter barley cultivars, reduces lodging (Chono
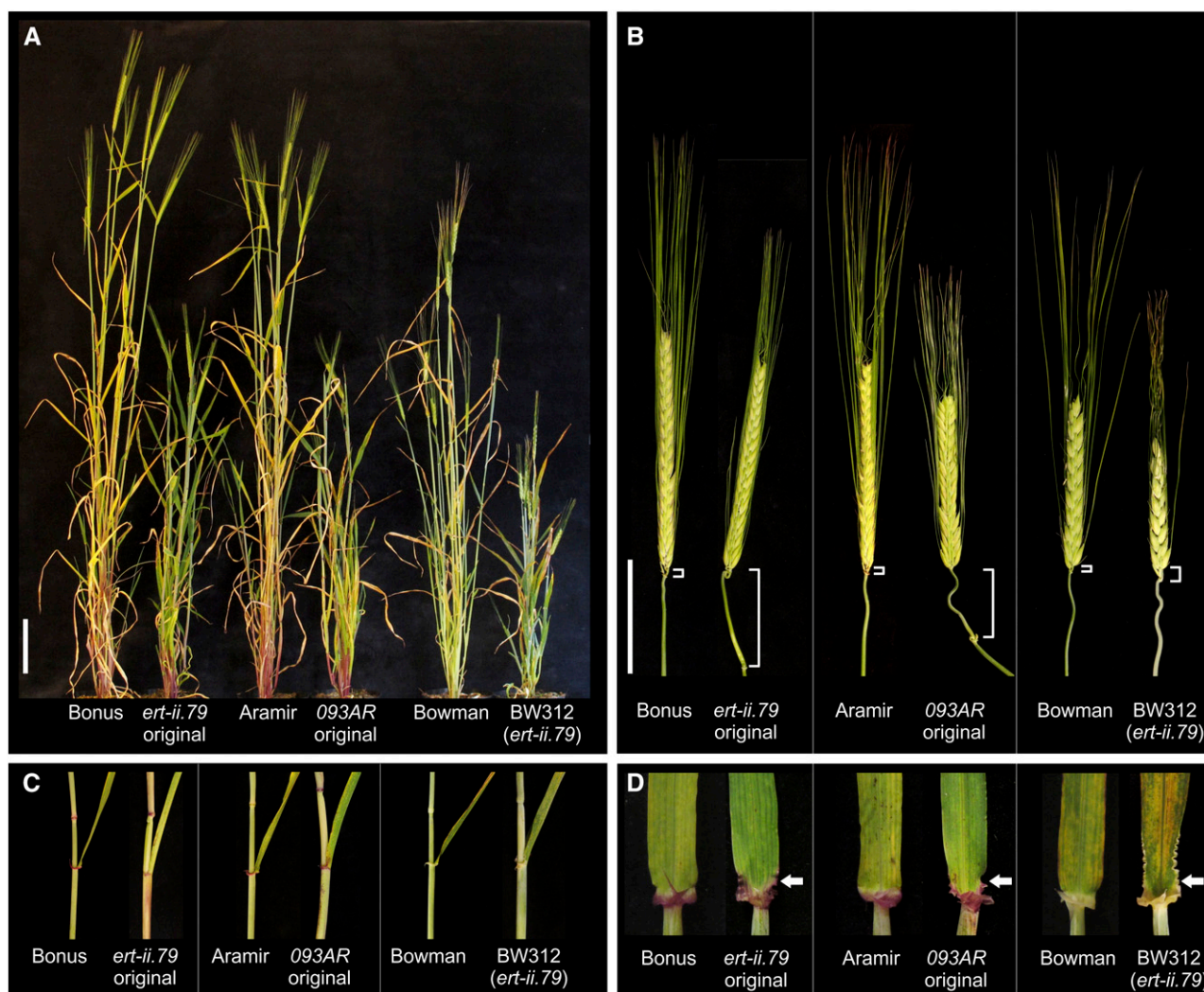
Figure 9. Phenotypic characterization of *uzu1.b* lines *ert-ii.79* (*uzu1.b* in cv Bonus), *093AR* (*uzu1.b* in cv Aramir), and BW312 (*uzu1.b* in cv Bowman). A, Gross morphology and general semidwarf phenotype. B, General spike phenotype with short awns, irregular rachis internodes, and elongated basal rachis internodes (a character not so pronounced in a cv Bowman genetic background). C, Erect leaf architecture. D, Undulating leaf margins of mutants compared with their respective parental cultivars. Scale bars = 10 cm in A and 5 cm in B.
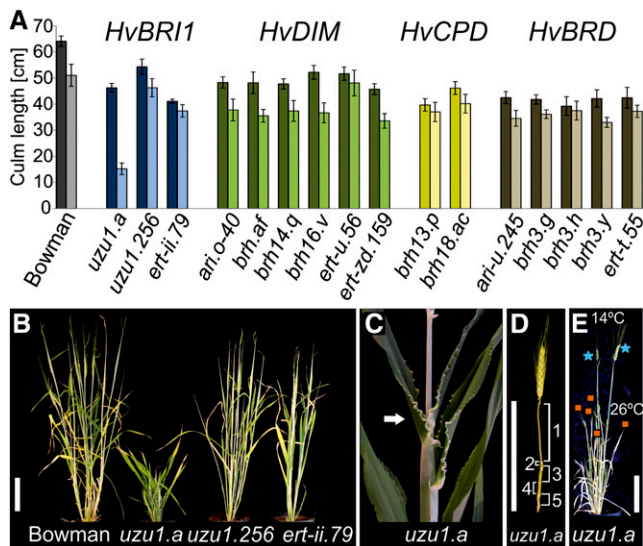
Figure 10. Temperature-responsive phenotypes of brassinosteroid mutants in the collection of cv Bowman near-isogenic lines compared with wild-type cv Bowman. A, Culm length of plants grown at 14°C (dark-colored bars) or 26°C (light-colored bars). B, *HvBRI1* mutants grown at 26°C. At high temperatures, elongation of *uzu1.a* culms is strongly reduced compared with cv Bowman and other brassinosteroid mutants. C and D, At 26°C, *uzu1.a* leaf margins are strongly undulating and internodes fail to elongate. E, Height reduction is partly neutralized by moving plants from warm temperature (26°C) to cool temperature (14°C). Squares and stars mark tillers developed at 26°C and 14°C, respectively. Scale bars = 10 cm. [See online article for color version of this figure.]

et al., 2003; Saisho et al., 2004) but shows sensitivity to elevated temperatures. We compared the near-isogenic line of *uzu1.a* with other brassinosteroid signaling and biosynthesis mutants grown at 14°C and 26°C. At 14°C, all mutants had an erect phenotype with height reduction ranging from strong (*brh3.h*, 61% of wild-type length) to weak semidwarfism (*uzu1.256*, 85%; Fig. 10). The average culm length of *uzu1.a* was 72% of the wild-type length. At 26°C, *uzu1.a* showed extreme dwarfing (29% of wild-type length) in contrast with the other mutants (65%–91%). When moved from 26°C to 14°C, already developed tillers remained short but new tillers grew taller (Fig. 10). We conclude that the temperature-sensitive phenotype is not associated with brassinosteroid or *HvBRI1* mutations in general, but is specific for the *uzu1.a* allele. We also measured the level of castasterone, the suggested end product of the brassinosteroid biosynthetic pathway in monocots (Kim et al., 2008). The highest level was found in *uzu1.a* grown at 26°C and in *ert-ii.79*, which are the signaling mutants with the strongest phenotype. This finding correlates well with the high levels of castasterone and brassinolide found in the Arabidopsis mutant *bri1-4* (Noguchi et al., 1999). Barley lines mutated in *HvBRD*, *HvCPD*, or *HvDIM* are deficient in brassinosteroid biosynthesis prior the formation of castasterone and thus had the lowest castasterone levels, as expected (Table I).

DISCUSSION

The Group of Brassinosteroid-Deficient Barley

The use of nitrogen fertilizers has an enormous impact on global cereal production and was a key component of the Green Revolution. Initially, the culms were not strong enough to support the heavy spikes of fertilized plants, which resulted in lodging and overall loss in yield. It was therefore necessary to combine the use of fertilizers with breeding of short-culm cultivars, which are less prone to lodging due to their compact and sturdy culms (Hedden, 2003). Thus far, only a few genes have been explored in short-culm cultivars, such as *Reduced height1* (*Rht1*), *Rht2*, and *Rht8* in wheat (Daoura et al., 2014), *semidwarf1* (*sd1*) in rice (Nagano et al., 2005), and *sdw1/denso* in barley (Hellewell et al., 2000). The known *Rht* gene products belong to the DELLA subgroup of the GRAS protein family, which are thought to function as transcriptional regulators and interfere with the signal transduction pathway of the gibberellin growth hormone (Pysh et al., 1999). By contrast, *sd1* and *sdw1/denso* are involved in the production of gibberellin because they encode gibberellin 20-oxidases of the biosynthetic pathway (Monna et al., 2002; Sasaki et al., 2002; Spielmeyer et al., 2002; Jia et al., 2009).

Plant height and cell elongation are also regulated by brassinosteroids (Vriet et al., 2012). The access to a collection of 160 short-culm mutants in a near-isogenic background and with roughly mapped mutant gene locations (Druka et al., 2011), in combination with in silico gene mapping using the latest barley genome resources (Mayer et al., 2011; The International Barley Genome Sequencing Consortium, 2012), enabled us to effectively discover brassinosteroid mutants by a reverse approach of phenotyping followed by genotyping. Unexpectedly, the identified semidwarf gene loci do not belong to the same barley complementation group but were described as *brh*, *uzu*, *ari*, and *ert* barley. The history of those mutants might explain this misleading pregrouping. The original mutations were induced and isolated in independent programs all over the world over a time period of several decades. Thus, mutagenic events were described and grouped by different barley researchers. An aggravating factor was that the plant material used for mutagenesis was dependent on

Table I. *Level of castasterone in barley near-isogenic lines carrying mutations in the brassinosteroid biosynthesis genes HvCPD, HvBRD, and HvDIM or the HvBRI1 gene encoding the brassinosteroid receptor*

Data are presented as the average ± SD unless otherwise indicated.

Near-Isogenic Line	Genotype	Castasterone
		pmol g leaf^{-1}
'Bowman'	Wild type	2.68 ± 0.40
BW084	*brh13.p* (*HvCPD*)	0.36 ± 0.06
BW091	*brh3.g* (*HvBRD*)	0.50 ± 0.06
BW333	*ert-zd.159* (*HvDIM*)	0.84 ± 0.29
BW033	*uzu1.256* (*HvBRI1*)	4.52 ± 0.53
BW312	*ert-ii.79* (*HvBRI1*)	9.39 ± 1.76
BW885	*uzu1.a* (*HvBRI1*)	7.43 ± 0.21
BW885 (26°C)	*uzu1.a* (*HvBRI1*)	10.31 ± 0.18

national cultivar preferences and, over time, was often changed. Thus, even though the isolated brassinosteroid barley mutants share the same characteristics, the connection between those original mutations was less obvious because the different parental backgrounds contribute other, distracting characters such as two- versus six-row spikes. Only the unification of the genetic background in the near-isogenic cv Bowman collection (Druka et al., 2011) helped to overcome this problem.

The short culm of brassinosteroid and gibberellin mutants is a trait of agronomic interest because it provides resistance to lodging. The erect and upright growth is unique to brassinosteroid mutants only and distinguishes them from gibberellin mutants. The erect leaves enhance light capture for photosynthesis, serve as a nitrogen reservoir for grain filling, and enable denser planting with a higher leaf surface per area of land (Sakamoto et al., 2006). It was shown that rice mutants deficient in brassinosteroid biosynthesis enhanced grain yield under conditions of dense planting (Sakamoto et al., 2006). Thus, brassinosteroid mutants provide additional traits for plant breeding that are not found in gibberellin mutants.

Interestingly, we only found mutations in three of approximately nine genes involved in brassinosteroid biosynthesis starting from episterol (Supplemental Fig. S1). The genes *HvDIM*, *HvCPD*, and *HvBRD* encode enzymes from different parts of the pathway. Mutations in the three genes show almost identical visible phenotypes, which suggests that loss of function of any other brassinosteroid biosynthesis gene should result in a similar plant architecture. However, it was found that a knockout of *DWARF4* (*DWF4*) in rice causes mild semidwarfism only (Sakamoto et al., 2006). Thus, it is possible that barley *HvDWF4* mutants were not isolated as short-culm mutants and therefore were not included in the mutant collections explored in this study. Similar, loss of function of a *CYP90*-like gene in rice resulted in severe dwarfism (Hong et al., 2003). Because severe barley dwarfs are not included in the collection of near-isogenic lines, it is possible that no suitable candidate plant for *HvCYP90D1* was present in our screen.

In addition, the existence of gene duplications in the barley genome or gene families with overlapping functions might explain why brassinosteroid biosynthesis mutants were only found in three genes. For example, *DWF4* appears to be represented by two very similar *DWF4*-like genes at almost identical positions on chromosome 4H at 60 cM in the physical map of barley (The International Barley Genome Sequencing Consortium, 2012). It is possible that only a double mutant might cause a brassinosteroid phenotype. Both *HvDWF4* genes overlap with the introgression regions of five near-isogenic lines with short-culm phenotypes, but without the unique combination of brassinosteroid features. Sequencing of *HvDWF4* from these lines did not reveal any mutations. Thus, it is likely that these lines are deficient in one or several genes linked to *HvDWF4*, but not involved in brassinosteroid biosynthesis or signaling.

Future studies on barley mutants deficient in other brassinosteroid-related genes will show whether we should regroup barley semidwarfs and introduce the group of brassinosteroid-deficient barley defined by the unique combination of phenotypic characters and genotypes described in this study. For example, screening for genetic polymorphism in known brassinosteroid-related genes in Targeting Induced Local Lesions in Genomes (TILLING) populations would reveal the phenotypic variation, which is not covered in this study due to the preset selection for short-culm mutants.

Induced Mutations in Barley

In our extensive screen for brassinosteroid mutants, we noted four interesting cases of identical mutations. In the first case, the mutants were induced by identical chemical treatment (*brh3.g*, *brh3.h*, and *brh3.i*), in the second case by different treatments (*ari-o.40*, *ari-o.43*, and *ari-o.143*). In each case, the mutants were induced in the same mutagenesis program, and thus we cannot exclude a mix-up of mutant accessions after the mutagenic treatment as it was suggested earlier for alleles of barley loci *praematurum-a* and *third outer glume1* (Houston et al., 2012; Zakhrabekova et al., 2012). Two other cases, however, strongly point toward an independent ancestry of identical mutations. Mutants *uzu1.b* (*093AR*) and *ert-ii.79* were induced in independent programs in different decades and countries. Here, we tested the genetic background and found a high level of polymorphism throughout the mutant genomes, strongly supporting their independent ancestry. In the other case, *brh3.y* and *ert-t.437*, silent mutations within *HvBRD*, in addition to the loss-of-function mutation, are clear evidence of an independent ancestry (Supplemental Data Set S1). Both cases invite speculation concerning mutation hotspots in barley, preferentially selected due to the strong brassinosteroid-mutant phenotype. Modern analytical techniques such as exome capture and genotyping-by-sequencing will help to clarify this finding and other cases in the near future.

Lodging-Resistant Barley in a Changing Climate

The barley *uzu1.a* mutant is known to have alterations in brassinosteroid signaling due to a nonsynonymous amino acid exchange in the BRI1 kinase domain (Chono et al., 2003). Although the *uzu1.a* gene modification has a long history in barley breeding, it remained exclusively in barley winter cultivars in Northeast Asia (Saisho et al., 2004). As shown in this study, the *uzu1.a* heat-sensitive reduction in plant height, severe in two-row spring barley grown in warmer climates, might be a reason why this haplotype did not spread globally during the Green Revolution. It is obvious that other alleles of *HvBRI1*, especially *uzu1.256* with its milder phenotype and without the pronounced temperature sensitivity of

uzu1.a, should be considered as more reliable alternatives for culm-length control in barley breeding. Interestingly, the *uzu1.a* mutation causes a change (His-857 to Arg) in a kinase surface domain (Bojar et al., 2014) that is not involved in ATP binding, nor does it interfere with the phosphorylation of the activation loop or with the position of the putative inhibitor BKI1 and SERK coreceptor binding site (Fig. 8, E and F). This is in agreement with the mild brassinosteroid phenotype we found in *uzu1.a* grown in moderate climate regimes. Mutations interfering with ATP binding, phosphorylation, or SERK interaction are known to cause drastic phenotypes in Arabidopsis and rice (Supplemental Fig. S8B), whereas mutations *uzu1.a* (at 14°C), *d61-10*, and *bri1-301*, all located within the same peripheral domain, result in mild phenotypes only (Fig. 8, E and F; Supplemental Fig. S8B). Here, exchanges of amino acid residues might not disturb the general structure of the kinase domain but instead interactions with other proteins of the signaling cascade, such as CONSTITUTIVE DIFFERENTIAL GROWTH1 or BRASSINOSTEROID-SIGNALING-KINASEs. However, because the temperature sensitivity is specific for *uzu1.a* only, it is very likely that the dynamic of BRI1 is affected by the modification of His-857. Such dynamic conformational changes might involve temporal stabilization by the cation-π interaction between His-857 and Phe-917 in the underlying α-helix (Fig. 8, E and F). A highly charged Arg-857 might push the equilibrium to the conformational state where the protein is stabilized in its inactive state via the cation-π interaction. Interestingly, it has been shown that elevated temperatures stabilize cation-π interactions (Prajapati et al., 2006). A temperature-dependent inactivation of BRI1 would be consistent with the temperature-sensitive dwarfism found in *uzu1.a*. We note that His-Phe or His-Tyr pairs are often arranged in very similar positions (His-[X_{57-59}]-Phe/Tyr) in many kinases, including plant receptor-like kinases (Supplemental Data Set S2).

The global temperature is currently rising and it has also been postulated that the climate may become more extreme with weather conditions that promote cereal lodging (Porter and Semenov, 2005; National Climate Assessment Development Advisory Committee, 2013). Accordingly, it would be desirable to have access to an increased repertoire of lodging-tolerance genes that also work under higher temperatures. The more than 20 temperature-insensitive mutations identified in this study can be transferred to elite cultivars by recurrent backcrosses. However, this is time-consuming and may bring unwanted variants through linked genes. An alternative approach is to screen for novel mutations directly induced in elite cultivars that already have favorable agronomic and grain-quality attributes. This can be done when the gene of interest is known. The visual phenotyping provides a fast and inexpensive method of identifying brassinosteroid mutants, thereby efficiently reducing the number of candidate genes to be analyzed in order to reveal the molecular cause of a short

and sturdy culm. An alternative approach is to create mutations through targeted mutagenesis and genome editing. However, these techniques are still in their infancy in barley (Wendt et al., 2013) and although it would be possible to create mutations without leaving any traces of foreign DNA in the resulting breeding lines, most countries regard such plants as genetically modified or legal decisions are pending. Regardless of the outcome of such decisions, public opinion has to show a positive acceptance to gene editing before it will be of economic importance. In view of these obstacles, we postulate that the more than 20 identified mutations and the visual identification of brassinosteroid-deficient short-culm phenotypes in induced mapping populations will remain attractive for many years. We propose that the phenotypic screening can be performed in any genetic background. We are currently screening a large number of uncharacterized short-culm mutants (including severe dwarfs) in order to identify mutations in other genes involved in brassinosteroid signaling and biosynthesis that were not revealed in this study.

MATERIALS AND METHODS

Plant Material and Growth Conditions

Barley (*Hordeum vulgare* 'Bowman') and other parental cultivars, cv Bowman near-isogenic mutant lines (Druka et al., 2011) and original mutant lines (Supplemental Data Set S1), F1 plants derived from allelism crosses, and an F2-mapping population from a cross between BW091 (*brh3.g*) × 'Bowman' were grown in a greenhouse at 18°C under 16-h-light/8-h-dark cycles. Temperature-dependent experiments were performed in a growth chamber at either 14°C or 26°C under 16-h-light/8-h-dark cycles. Light intensity was set to a photon flux of 300 μmol m^{-2} s^{-1}.

For propiconazole treatments, barley seeds of cv Bowman' were imbibed and germinated on filter paper drenched with the respective propiconazole dilutions in water. Seeds were transplanted in soil after radicle emergence. For propiconazole treatments, barley plants were grown under greenhouse conditions at 26°C (day) and 18°C (night). Single plants were grown in 20-cm-wide pots in 1:1 (v/v) mixtures of Turface Athletics MVP (Profile Products) and Pro-Mix-BX with microrise (Premier Horticulture). Plants were fertilized with 0.02% (v/v) Miracle-Gro Excel (Scotts) adjusted to pH 6.0 following the manufacturer's recommendations. The watering solution was supplemented with 500 μM propiconazole solution using the commercial fungicide formulation Banner Maxx (Syngenta). Propiconazole treatments were applied during each watering cycle via soil drench. At full development of spikes, morphometric data were gathered and photographs were taken.

Plant seeds are either available from the Nordic Genetic Resource Center (http://www.nordgen.org) or from the National Small Grains Collection (http://www.ars.usda.gov). Seeds of mutant *brh.af* were kindly provided by Andy Kleinhofs.

Allelism Crosses

Allelism tests were performed through crosses between barley accessions carrying mutations in identical brassinosteroid-related genes. Plants were grown in a greenhouse as described above, emasculated, and pollinated within 3 d. The following cv Bowman near-isogenic lines (Druka et al., 2011) were used for allelism tests concerning *HvBRD*, *HvDIM* and *HvCPD*: BW031 (*ari-u.245*) × BW094 (*brh3.y*), BW053 (*ari-o.40*) × BW072 (*brh.af*), BW053 (*ari-o.40*) × BW085 (*brh14.q*), BW053 (*ari-o.40*) × BW325 (*ert-u.56*), BW053 (*ari-o.40*) × BW333 (*ert-zd.159*), BW333 (*ert-zd.159*) × BW087 (*brh16.v*), and BW084 (*brh13.p*) × BW089 (*brh18.ac*). In addition, we crossed the original mutant accession *ari-o.40* with *ari-o.297*, *ari-o.301*, *ari-o.304*, and *ari-o.306*. In the case of *HvBRI1*, mutant *uzu1.c* (*R710K*) was crossed to both BW885 (*uzu1.a*) and 093AR (*uzu1.b*). F1 progenies of all crosses were genotyped to confirm successful crossings, and were grown to maturity for phenotypic

analysis. Allelism tests between other mutants identified in this study are described elsewhere (Dahleen et al., 2005; Franckowiak and Lundqvist, 2012).

Leaf-Segment Unrolling and Leaf Lamina Inclination Assay

Leaf-segment unrolling tests were performed as described in Chono et al. (2003) and Gruszka et al. (2011a). The rate of leaf-segment unrolling was calculated according to Wada et al. (1985). For leaf lamina inclination tests, plants were grown in vermiculite until the first leaf protruded 2 cm above the coleoptile. One microliter of 2 mg mL^{-1} brassinolide (24-epi-brassinolide; Sigma-Aldrich Chemie) solved in 96% (v/v) ethanol was added to the tip of the barley seedlings. The angle between the first leaf and the second leaf was measured when the second leaf emerged.

Quantification of Castasterone Levels

Isolation and identification of the brassinosteroid biosynthetic intermediate castasterone was performed according to a modified protocol described in Swaczynová et al. (2007) and Janeczko et al. (2010). All plants were grown for 14 d at 17°C, except BW885, which was also grown at 26°C. For each genotype, measurements were performed in three replicates. The leaf material (2 g fresh weight) was homogenized in 20 mL of 80% (v/v) cold methanol. After centrifugation, the supernatant was enriched in deuterium-labeled brassinosteroids (internal standards) and passed through a Strata X column (Phenomenex). The bound fraction was eluted with acetonitrile and evaporated to dryness. Brassinosteroids were determined by ultra-HPLC with tandem mass spectrometry.

In Silico Gene Mapping

Coding DNA sequences and protein sequences of Arabidopsis (*Arabidopsis thaliana*) genes *STE1* (AT3G02580), *DWF5* (AT1G50430), *DIM/DWF1* (AT3G19820), *DET2* (AT2G38050), *CYP90B1/DWF4* (AT3G50660), *CYP90C1/ROT3* (AT4G36380), *CYP90D1* (AT3G13730), *CYP90A1/CPD* (AT5G05690), *CYP85A/BR6ox/BRD1* (AT5G38970), or *BRD2* (AT3G30180) and rice (*Oryza sativa*) *CYP724B1/DWF11* (LOC_Os04g39430) were used as probes to identify full-length barley gene and peptide sequences via the IPK Barley BLAST Server of the Leibniz Institute of Plant Genetics and Crop Plant Research (http://webblast.ipk-gatersleben.de/). Inferred and anchored positions of barley high-confidence genes were extracted from the barley genome zipper (Mayer et al., 2011) and the barley genome map (The International Barley Genome Sequencing Consortium, 2012), respectively. Barley and Arabidopsis peptide sequences were aligned using Clustal Omega software (http://www.ebi.ac.uk/Tools/msa/clustalo/).

Resequencing of *HvBRD*, *HvCPD*, *HvDIM*, *HvDWF4*, and *HvBRI1*

Genomic DNA was extracted from green leaf material using the REDExtract-N-Amp Plant PCR Kit (Sigma-Aldrich) according to the manufacturer's instructions. Green leaves of an F2-mapping population were sampled in 96-well format and genomic DNA was isolated using a Freedom EVO 200 robot (Tecan Group). PCR amplifications of AK372445 (*HvBRD*), MLOC_10658 (*HvCPD*), MLOC_52405 (*HvDIM*), AK355174 (*HvDWF4*), and MLOC_5176 (*HvBRI1*) were performed according to the manufacturer's protocol (REDExtract-N-Amp PCR ReadyMix; Sigma-Aldrich).

PCRs for *HvBRD* fragments 1, 2, and 5 were performed for 42 cycles (initial denaturation at 94°C/3 min followed by three cycles of 94°C/45 s, 61.5°C/45 s, and 72°C/90 s for extension; followed by three cycles of 94°C/45 s, 59.5°C/45 s, and 72°C/90 s for extension; and followed by 36 cycles of 94°C/45 s, primer pair-dependent annealing temperature/45 s, and 72°C/90 s for extension, with a final extension step of 72°C/10 min). PCRs for *HvBRD* fragments 3 and 4 were performed for 30 cycles (initial denaturation at 94°C/3 min followed by 30 cycles of 94°C/45 s, 54.5°C/45 s, and 72°C/105 s for extension, with a final extension step of 72°C/10 min). PCRs for *HvBRI1* were performed using the protocol published in Gruszka et al. (2011b). PCRs for *HvCPD* were performed for 37 cycles (initial denaturation at 94°C/3 min followed by 37 cycles of 94°C/45 s, 54.5°C/45 s, and 72°C/90 s for extension, with a final extension step of 72°C/10 min). PCRs for *HvDIM* were performed for 40 cycles (initial denaturation at 94°C/3 min followed by 40 cycles of 94°C/30 s, 59°C/30 s, and 72°C/60–90 s for extension, with a final extension step of 72°C/10 min). PCRs for *HvDWF4* were performed for 42 cycles (initial denaturation at 94°C/3 min

followed by three cycles of 94°C/45 s, 58°C/45 s, and 72°C/90 s for extension; followed by three cycles of 94°C/45 s, 56°C/45 s, and 72°C/90 s for extension; and followed by 36 cycles of 94°C/45 s, 54.5°C/45 s, and 72°C/90 s for extension, with a final extension step of 72°C/10 min). Primer sequences including specific annealing temperatures used for PCR amplifications are listed and described in Supplemental Data Set S3.

PCR products were resolved by agarose gel electrophoresis (GenAgaroseLE; GENAXXON Bioscience) and visualized after ethidium bromide staining. PCR products were purified using the NucleoSpin Gel and PCR Clean-Up Kit (Macherey-Nagel) according to the manufacturer's instructions. Purified PCR products were sequenced by StarSEQ.

Molecular Analysis of *uzu1.b* Mutants *ert-ii.79* and *093AR*

Genomic DNA of two *uzu1.b* alleles, *ert-ii.79* and *093AR*, and of their respective parents, 'Bonus' and 'Aramir,' was isolated from green leaf material using the micro cetyl trimethylammonium bromide protocol described in Gruszka et al. (2011b). For this analysis, the AFLP marker technique was applied. Two parental varieties were compared with each other. Similarly, AFLP band patterns were compared between the mutants and mutants also were reciprocally compared with the parental varieties. During the analysis, on average, more than 380 AFLP bands were scored for each comparison.

Mutagenesis and TILLING Screen of a Barley M2 Generation

The doubled-haploid line H930-36 was developed from the F1 generation of a cross between barley 'Klages' and variety Mata. H930-36 was mutagenized by chemical treatment with *N*-methyl-*N*-nitrosourea at a dose of 1.5 mM/3 h. Then, 950 individual plants of the M2 generation were grown in the field and phenotyped at maturity. Leaf material of individual plants was harvested, dried in Silica Gel Type III (Sigma-Aldrich), and ground with an electric grinder (Retsch). DNA was extracted using the micro cetyl trimethylammonium bromide protocol (Gruszka et al., 2011b) and genotypes were analyzed using the TILLING approach described in Kurowska et al. (2012). Two fragments of the *HvBRI1* spanning the gene region from 1,639 to 2,994 bp (Supplemental Fig. S8B), were analyzed for sequence alterations.

Anatomical and Microscopic Analysis

For histological assays of 2-mm root segments of 5-d-old barley seedlings, conventional fixation, substitution, and embedding procedures were performed as described elsewhere (Marzec et al., 2013). Semithin sections (approximately 2 μm thick) were stained for 2 min with 1% (w/v) methylene blue/1% (w/v) Azur II in 1% (w/v) aqueous borax at 60°C before light microscopic examination with a Zeiss Axiovert 135 microscope. In order to analyze the root architecture, one seed per plastic tube (50-cm length and 40-mm diameter) was sown in vermiculite. Roots of 18-d-old plants were analyzed using a standard Epson scanner and WinRhizo software (Regent Instruments).

Sequence data from this article can be found in the GenBank/EMBL data libraries under accession numbers KF318307 (*HvDIM*), KF318308 (*HvBRD*), and KF360233 (*HvCPD*).

Supplemental Data

The following materials are available in the online version of this article.

Supplemental Figure S1. The brassinosteroid biosynthetic pathway as found in Arabidopsis.

Supplemental Figure S2. Anatomical and microscopic analysis of seedlings of cv Bowman near-isogenic lines BW031 (*ari-u.245*), BW084 (*brh13.p*), BW333 (*ert-zd.159*), and BW312 (*ert-ii.79*).

Supplemental Figure S3. Leaf-inclination assay of seedlings of cv Bowman near-isogenic lines BW031 (*ari-u.245*), BW084 (*brh13.p*), BW312 (*ert-ii.79*), and BW333 (*ert-zd.159*).

Supplemental Figure S4. Alignments of brassinosteroid-biosynthesis enzymes from Arabidopsis and barley.

Supplemental Figure S5. In silico mapping and detailed analysis of conserved amino acid residues of *HvBRD*.

Supplemental Figure S6. In silico mapping and detailed analysis of conserved amino acid residues of *HvCPD*.

Supplemental Figure S7. In silico mapping and detailed analysis of conserved amino acid residues of *HvDIM*.

Supplemental Figure S8. In silico mapping and detailed analysis of conserved amino acid residues of *HvBRI1*.

Supplemental Data Set S1. Overview and description of analyzed barley mutant accessions and parental cultivars.

Supplemental Data Set S2. Examples of kinases with a cation-Pi His-[X_{57-59}]-Phe/Tyr motif.

Supplemental Data Set S3. Primers used for amplification of the *HvBRD*, *HvBRI1*, *HvCPD*, *HvDIM*, and *HvDWF4* genomic DNA sequences.

LITERATURE CITED

Bai MY, Shang JX, Oh E, Fan M, Bai Y, Zentella R, Sun TP, Wang ZY (2012) Brassinosteroid, gibberellin and phytochrome impinge on a common transcription module in *Arabidopsis*. Nat Cell Biol **14:** 810–817

Bajguz A, Tretyn A (2003) The chemical characteristic and distribution of brassinosteroids in plants. Phytochemistry **62:** 1027–1046

Bojar D, Martinez J, Santiago J, Rybin V, Bayliss R, Hothorn M (2014) Crystal structures of the phosphorylated BRI1 kinase domain and implications for brassinosteroid signal initiation. Plant J **78:** 31–43

Bosshard HR, Marti DN, Jelesarov I (2004) Protein stabilization by salt bridges: concepts, experimental approaches and clarification of some misunderstandings. J Mol Recognit **17:** 1–16

Chandler PM, Harding CA (2013) 'Overgrowth' mutants in barley and wheat: new alleles and phenotypes of the 'Green Revolution' *DELLA* gene. J Exp Bot **64:** 1603–1613

Chono M, Honda I, Zeniya H, Yoneyama K, Saisho D, Takeda K, Takatsuto S, Hoshino T, Watanabe Y (2003) A semidwarf phenotype of barley uzu results from a nucleotide substitution in the gene encoding a putative brassinosteroid receptor. Plant Physiol **133:** 1209–1219

Dahleen LS, Vander Wal LJ, Franckowiak JD (2005) Characterization and molecular mapping of genes determining semidwarfism in barley. J Hered **96:** 654–662

Daoura BG, Chen L, Du Y, Hu YG (2014) Genetic effects of dwarfing gene *Rht-5* on agronomic traits in common wheat (*Triticum aestivum* L.) and QTL analysis on its linked traits. Field Crops Res **156:** 22–29

Druka A, Franckowiak J, Lundqvist U, Bonar N, Alexander J, Houston K, Radovic S, Shahinnia F, Vendramin V, Morgante M, et al (2011) Genetic dissection of barley morphology and development. Plant Physiol **155:** 617–627

Franckowiak JD, Lundqvist U (2012) Descriptions of barley genetic stocks for 2012. Barley Genet Newsl **42:** 36–792

Fujioka S, Noguchi T, Takatsuto S, Yoshida S (1998) Activity of brassinosteroids in the dwarf rice lamina inclination bioassay. Phytochemistry **49:** 1841–1848

Greeve I, Hermans-Borgmeyer I, Brellinger C, Kasper D, Gomez-Isla T, Behl C, Levkau B, Nitsch RM (2000) The human DIMINUTO/DWARF1 homolog seladin-1 confers resistance to Alzheimer's disease-associated neurodegeneration and oxidative stress. J Neurosci **20:** 7345–7352

Gruszka D, Szarejko I, Maluszynski M (2011a) Identification of barley *DWARF* gene involved in brassinosteroid synthesis. Plant Growth Regul **65:** 343–358

Gruszka D, Szarejko I, Maluszynski M (2011b) New allele of *HvBRI1* gene encoding brassinosteroid receptor in barley. J Appl Genet **52:** 257–268

Hartwig T, Corvalan C, Best NB, Budka JS, Zhu JY, Choe S, Schulz B (2012) Propiconazole is a specific and accessible brassinosteroid (BR) biosynthesis inhibitor for *Arabidopsis* and maize. PLoS ONE **7:** e36625

Hay A, Hake S (2004) The dominant mutant *Wavy auricle in blade1* disrupts patterning in a lateral domain of the maize leaf. Plant Physiol **135:** 300–308

Hedden P (2003) The genes of the Green Revolution. Trends Genet **19:** 5–9

Hellewell KB, Rasmusson DC, Gallo-Meagher G (2000) Enhancing yield in semidwarf barley. Crop Sci **40:** 352–358

Helliwell CA, Chandler PM, Poole A, Dennis ES, Peacock WJ (2001) The CYP88A cytochrome P450, *ent*-kaurenoic acid oxidase, catalyzes three steps of the gibberellin biosynthesis pathway. Proc Natl Acad Sci USA **98:** 2065–2070

Honda I, Zeniya H, Yoneyama K, Chono M, Kaneko S, Watanabe Y (2003) *Uzu* mutation in barley (*Hordeum vulgare* L.) reduces the leaf unrolling response to brassinolide. Biosci Biotechnol Biochem **67:** 1194–1197

Hong Z, Jin H, Tzfira T, Li J (2008) Multiple mechanism-mediated retention of a defective brassinosteroid receptor in the endoplasmic reticulum of *Arabidopsis*. Plant Cell **20:** 3418–3429

Hong Z, Ueguchi-Tanaka M, Umemura K, Uozu S, Fujioka S, Takatsuto S, Yoshida S, Ashikari M, Kitano H, Matsuoka M (2003) A rice brassinosteroid-deficient mutant, *ebisu dwarf* (*d2*), is caused by a loss of function of a new member of cytochrome P450. Plant Cell **15:** 2900–2910

Hothorn M, Belkhadir Y, Dreux M, Dabi T, Noel JP, Wilson IA, Chory J (2011) Structural basis of steroid hormone perception by the receptor kinase BRI1. Nature **474:** 467–471

Houston K, Druka A, Bonar N, Macaulay M, Lundqvist U, Franckowiak J, Morgante M, Stein N, Waugh R (2012) Analysis of the barley bract suppression gene *Trd1*. Theor Appl Genet **125:** 33–45

Houston K, McKim SM, Comadran J, Bonar N, Druka I, Uzrek N, Cirillo E, Guzy-Wrobelska J, Collins NC, Halpin C, et al (2013) Variation in the interaction between alleles of *HvAPETALA2* and microRNA172 determines the density of grains on the barley inflorescence. Proc Natl Acad Sci USA **110:** 16675–16680

Janeczko A, Biesaga–Kościelniak J, Oklešťková J, Filek M, Dziurka M, Szarek-Łukaszewska G, Kościelniak J (2010) Role of 24-epibrassinolide in wheat production: physiological effects and uptake. J Agron Crop Sci **196:** 311–321

Jia Q, Zhang J, Westcott S, Zhang XQ, Bellgard M, Lance R, Li C (2009) GA-20 oxidase as a candidate for the semidwarf gene *sdw1/denso* in barley. Funct Integr Genomics **9:** 255–262

Kim BK, Fujioka S, Takatsuto S, Tsujimoto M, Choe S (2008) Castasterone is a likely end product of brassinosteroid biosynthetic pathway in rice. Biochem Biophys Res Commun **374:** 614–619

Kim TW, Wang ZY (2010) Brassinosteroid signal transduction from receptor kinases to transcription factors. Annu Rev Plant Biol **61:** 681–704

Kurowska M, Labocha-Pawłowska A, Gnizda D, Maluszynski M, Szarejko I (2012) Molecular analysis of point mutations in a barley genome exposed to MNU and gamma rays. Mutat Res **738-739:** 52–70

Li J, Chory J (1997) A putative leucine-rich repeat receptor kinase involved in brassinosteroid signal transduction. Cell **90:** 929–938

Marzec M, Melzer M, Szarejko I (2013) Asymmetric growth of root epidermal cells is related to the differentiation of root hair cells in *Hordeum vulgare* (L.). J Exp Bot **64:** 5145–5155

Mayer KF, Martis M, Hedley PE, Simková H, Liu H, Morris JA, Steuernagel B, Taudien S, Roessner S, Gundlach H, et al (2011) Unlocking the barley genome by chromosomal and comparative genomics. Plant Cell **23:** 1249–1263

Monna L, Kitazawa N, Yoshino R, Suzuki J, Masuda H, Maehara Y, Tanji M, Sato M, Nasu S, Minobe Y (2002) Positional cloning of rice semidwarfing gene, *sd-1*: rice "green revolution gene" encodes a mutant enzyme involved in gibberellin synthesis. DNA Res **9:** 11–17

Nagano H, Onishi K, Ogasawara M, Horiuchi Y, Sano Y (2005) Genealogy of the "Green Revolution" gene in rice. Genes Genet Syst **80:** 351–356

National Climate Assessment Development Advisory Committee (2013) The U.S. Global Change Research Program http://ncadac.globalchange.gov/

Noguchi T, Fujioka S, Choe S, Takatsuto S, Yoshida S, Yuan H, Feldmann KA, Tax FE (1999) Brassinosteroid-insensitive dwarf mutants of Arabidopsis accumulate brassinosteroids. Plant Physiol **121:** 743–752

Pettersen EF, Goddard TD, Huang CC, Couch GS, Greenblatt DM, Meng EC, Ferrin TE (2004) UCSF Chimera—a visualization system for exploratory research and analysis. J Comput Chem **25:** 1605–1612

Porter JR, Semenov MA (2005) Crop responses to climatic variation. Philos Trans R Soc Lond B Biol Sci **360:** 2021–2035

Prajapati RS, Sirajuddin M, Durani V, Sreeramulu S, Varadarajan R (2006) Contribution of cation-pi interactions to protein stability. Biochemistry **45:** 15000–15010

Pysh LD, Wysocka-Diller JW, Camilleri C, Bouchez D, Benfey PN (1999) The GRAS gene family in *Arabidopsis*: sequence characterization and basic expression analysis of the *SCARECROW-LIKE* genes. Plant J **18:** 111–119

Rajkumara S (2008) Lodging in cereals. Agric Rev **29:** 55–60

Saisho D, Tanno K, Chono M, Honda I, Kitano H, Takeda K (2004) Spontaneous brassinolide-insensitive barley mutants "*uzu*" adapted to East Asia. Breed Sci **54:** 409–416

Sakamoto T, Morinaka Y, Ohnishi T, Sunohara H, Fujioka S, Ueguchi-Tanaka M, Mizutani M, Sakata K, Takatsuto S, Yoshida S, et al (2006) Erect leaves caused by brassinosteroid deficiency increase biomass production and grain yield in rice. Nat Biotechnol **24:** 105–109

Santiago J, Henzler C, Hothorn M (2013) Molecular mechanism for plant steroid receptor activation by somatic embryogenesis co-receptor kinases. Science **341:** 889–892

Sasaki A, Ashikari M, Ueguchi-Tanaka M, Itoh H, Nishimura A, Swapan D, Ishiyama K, Saito T, Kobayashi M, Khush GS, et al (2002) Green revolution: a mutant gibberellin-synthesis gene in rice. Nature **416:** 701–702

She J, Han Z, Kim TW, Wang J, Cheng W, Chang J, Shi S, Wang J, Yang M, Wang ZY, et al (2011) Structural insight into brassinosteroid perception by BRI1. Nature **474:** 472–476

Shimada Y, Fujioka S, Miyauchi N, Kushiro M, Takatsuto S, Nomura T, Yokota T, Kamiya Y, Bishop GJ, Yoshida S (2001) Brassinosteroid-6-oxidases from Arabidopsis and tomato catalyze multiple C-6 oxidations in brassinosteroid biosynthesis. Plant Physiol **126:** 770–779

Spielmeyer W, Ellis MH, Chandler PM (2002) Semidwarf (*sd-1*), "green revolution" rice, contains a defective gibberellin 20-oxidase gene. Proc Natl Acad Sci USA **99:** 9043–9048

Sun Y, Han Z, Tang J, Hu Z, Chai C, Zhou B, Chai J (2013) Structure reveals that BAK1 as a co-receptor recognizes the BRI1-bound brassinolide. Cell Res **23:** 1326–1329

Swaczynová J, Novák O, Hauserová E, Funksová K, Šíša M, Strnad M (2007) New techniques for estimation of naturally occurring brassinosteroids. J Plant Growth Regul **26:** 1–14

The International Barley Genome Sequencing Consortium (2012) A physical, genetic and functional sequence assembly of the barley genome. Nature **491:** 711–716

Wada K, Kondo H, Marumo S (1985) A simple bioassay for brassinosteroids: A wheat leaf-unrolling test. Agric Biol Chem **49:** 2249–2251

Wendt T, Holm PB, Starker CG, Christian M, Voytas DF, Brinch-Pedersen H, Holme IB (2013) TAL effector nucleases induce mutations at a pre-selected location in the genome of primary barley transformants. Plant Mol Biol **83:** 279–285

Vriet C, Russinova E, Reuzeau C (2012) Boosting crop yields with plant steroids. Plant Cell **24:** 842–857

Zakhrabekova S, Gough SP, Braumann I, Müller AH, Lundqvist J, Ahmann K, Dockter C, Matyszczak I, Kurowska M, Druka A, et al (2012) Induced mutations in circadian clock regulator *Mat-a* facilitated short-season adaptation and range extension in cultivated barley. Proc Natl Acad Sci USA **109:** 4326–4331